Journal of Inorganic Biochemistry 134 (2014) 66–75

Contents lists available at ScienceDirect

Journal of Inorganic Biochemistry

journal homepage: www.elsevier.com/locate/jinorgbio

Synthesis, characterization, thermal and DNA-binding properties of new zinc complexes with 2-hydroxyphenones

Emina Mrkalić [a,b], Ariadni Zianna [a], George Psomas [a], Maria Gdaniec [c], Agnieszka Czapik [c], Evdoxia Coutouli-Argyropoulou [d], Maria Lalia-Kantouri [a,*]

[a] Department of General and Inorganic Chemistry, Faculty of Chemistry, Aristotle University of Thessaloniki, GR-54124 Thessaloniki, Greece
[b] Institute of Chemistry, Faculty of Sciences, University of Kragujevac, 34000 Kragujevac, Serbia
[c] Faculty of Chemistry, Adam Mickiewicz University, 61614 Poznan, Poland
[d] Department of Organic Chemistry and Biochemistry, Faculty of Chemistry, Aristotle University of Thessaloniki, GR-54124 Thessaloniki, Greece

ARTICLE INFO

Article history:
Received 11 November 2013
Received in revised form 16 December 2013
Accepted 24 January 2014
Available online 3 February 2014

Keywords:
Zinc complexes
2-Hydroxyphenones
Crystal structure
Thermal behavior
Interaction with calf-thymus DNA
Competitive studies with ethidium bromide

ABSTRACT

The neutral mononuclear zinc complexes with 2-hydroxyphenones (ketoH) having the formula $[Zn(keto)_2(H_2O)_2]$ and $[Zn(keto)_2(enR)]$, where enR stands for a N,N'-donor heterocyclic ligand such as 2,2′-bipyridine (bipy), 1,10-phenanthroline (phen) or 2,2′-dipyridylamine (dpamH), have been synthesized and characterized by IR, UV and ^{1}H NMR spectroscopies. The 2-hydroxyphenones are chelated to the metal ion through the phenolate and carbonyl oxygen atoms. The crystal structures of [bis(2-hydroxy-4-methoxy-benzophenone)(2,2′-bipyridine)zinc(II)] dimethanol solvate and [bis(2-hydroxy-benzophenone)(2,2′-bipyridine)zinc(II)] dimethanol solvate have been determined by X-ray crystallography. The thermal stability of the zinc complexes has been investigated by simultaneous TG/DTG–DTA technique. The ability of the complexes to bind to calf-thymus DNA (CT DNA) has been studied by UV-absorption and fluorescence emission spectroscopy as well as viscosity measurements. UV studies of the interaction of the complexes with DNA have shown that they can bind to CT DNA and the corresponding binding constants to DNA have been calculated and evaluated. The complexes most probably bind to CT DNA via intercalation as concluded by studying the viscosity of a DNA solution in the presence of the complexes. Competitive studies with ethidium bromide (EB) have shown that the reported complexes can displace the DNA-bound EB, suggesting strong competition with EB for the intercalation site.

1. Introduction

Zinc is an essential trace element for the growth and development in all forms of life and has presented beneficial, therapeutic and preventive effects on infectious diseases [1,2], being the second most abundant trace metal in the human body [3]. Zinc is not only an essential cofactor with catalytic, structural or regulatory role in a plethora of enzymes but also its complexes are often used as drugs [4–6]. In the literature, diverse zinc complexes showing a noteworthy biological activity have been structurally characterized, including zinc complexes with drugs used for the treatment of Alzheimer disease [7] and others showing bactericidal [8], anticonvulsant [9], antidiabetic [5], anti-inflammatory [10], antimicrobial [11], antioxidant [12] and cytotoxic [13–15] activity.

Benzophenone and its derivatives have been widely used in many commercial products, e.g. sunscreens, cosmetics and plastic surface coatings, because of their ability to absorb and dissipate ultraviolet light A (400–315 nm) [16–18]. Besides their important commercial interest, a large number of studies have been carried out in regard to the pharmacological effects of benzophenone and its derivatives explaining the expanding interest for their use. These compounds have been effective *in vitro* and *in vivo* for the treatment of anaphylaxis, androgenesis, inflammation, malaria, tuberculosis and virus [18–26]; they are also considered as inhibitors of HIV, farnesyltransferase and reverse transcriptase [27–29]. On the other side, benzophenones may be absorbed through human skin resulting in a possible bioaccumulation in the human body [30]. They have also been found to be endocrine disrupting chemicals (EDCs) with some hydroxylated benzophenones, such as the 2- and 4-hydroxylated derivatives, showing both estrogenic and antiandrogenic activities [18]. Additionally, hepatotoxicity [31] and some incidents of photoallergic reactions in patients with suspected clinical photosensitivity [32] have been reported. Keeping in mind these controversial effects, it is of important significance the preparation of new benzophenone compounds (including their complexes) which may show enhanced biological activity in comparison to the existing compounds.

We have initiated the synthesis and characterization of transition metal complexes with carbonyl compounds derived from salicylaldehyde and benzophenone [33–37]. Within this context, the neutral mononuclear zinc complexes with two 2-hydroxybenzophenones (abbreviated as ketoH), 2-hydroxybenzophenone (=bpoH, 2-OH-benzophenone) and 2-hydroxy-4-methoxybenzophenone (=opoH, 2-OH-4-MeO-

* Corresponding author. Tel./fax: +30 2310 997844.
E-mail address: lalia@chem.auth.gr (M. Lalia-Kantouri).

0162-0134/$ – see front matter © 2014 Elsevier Inc. All rights reserved.
http://dx.doi.org/10.1016/j.jinorgbio.2014.01.019

benzophenone, commercially known as benzophenone 3; see Scheme 1(A)) were prepared and characterized. Complexes **1** and **5** of the formula $[Zn(keto)_2(H_2O)_2]$ were synthesized in the absence of the N,N′-donor heterocyclic ligand (enR), whereas complexes **2**–**4** and **6**–**8** of the formula $[Zn(keto)_2(enR)]$ were prepared in the presence of 2,2′-bipyridine (bipy) (**2** and **6**), 1,10-phenanthroline (phen) (**3** and **7**) or 2,2′-dipyridylamine (dpamH) (**4** and **8**). The crystal structures of the solvated complexes **2** and **6** have been determined by X-ray crystallography. The thermal stability and decomposition mode for five of the compounds were studied in nitrogen atmosphere by using the simultaneous technique (TG/DTG–DTA).

The interaction of transition metal complexes with DNA has been in the center of scientific interest for many years, mainly due to their versatile applications in cancer research and nucleic acid chemistry [38–42]. Nevertheless, as revealed by a thorough search of the literature, the interaction of DNA with 2-hydroxy-benzophenones and their metal complexes has not been studied up to now. Therefore, in the general context of the research of potential metallodrugs as well as biological importance of zinc, interaction of DNA with the easily available ketoH ligands, opoH and bpoH, and their Zn complexes **1**–**8**, was deemed worthy of extensive studies. As continuation of our earlier research [33], the ability of opoH, bpoH and complexes **1**–**8** to bind to calf-thymus (CT) DNA has been investigated by (i) UV spectroscopic titration where the binding constants K_b of the compounds to CT DNA have been calculated, (ii) measurements of the viscosity of DNA solution in the presence of increasing amounts of the compounds (ketoHs and their complexes) and (iii) competitive binding titration with the classic intercalator ethidium bromide (EB) performed by fluorescence emission spectroscopy in order to assess the ability of the compounds to displace EB from the EB–DNA complex as an indirect proof of a potential intercalative binding mode.

2. Experimental

2.1. Materials

The ketoH ligands (opoH and bpoH), the amines enR (bipy, phen and dpamH), NaCl, CH_3ONa, $Zn(NO_3)_2.6H_2O$, trisodium citrate, CT DNA and EB were obtained as reagent grade from Sigma-Aldrich Co and used as received. Solvents for preparation and physical measurements of "extra pure" grade were obtained from Merck and used without further purification. DNA stock solution was prepared by dilution of CT DNA to buffer (containing 150 mM NaCl and 15 mM trisodium citrate at pH 7.0) followed by exhaustive stirring at 4 °C for 3 days, and kept at 4 °C for no longer than a week. The stock solution of CT DNA gave a ratio of UV absorbances at 260 and 280 nm (A_{260}/A_{280}) of 1.87, indicating that the DNA was sufficiently free of protein contamination. The DNA concentration per base pair was determined after 1:20 dilution by the UV absorbance at 260 nm using $\varepsilon = 6600\ M^{-1}\ cm^{-1}$ [43].

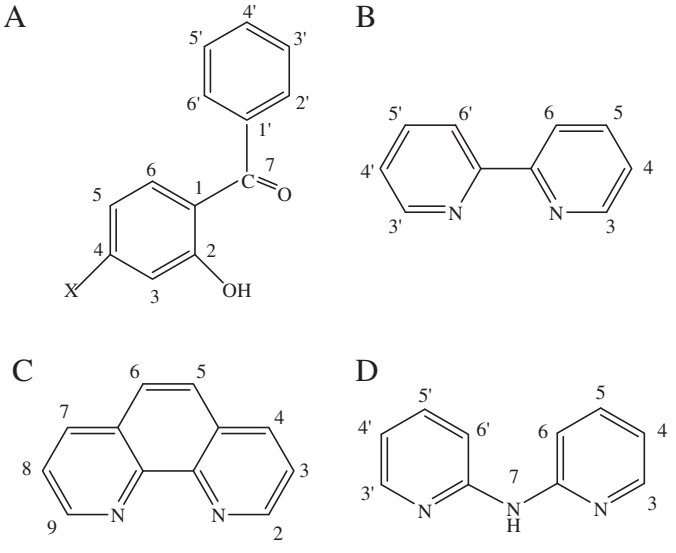

Scheme 1. (A) The 2-hydroxyphenone ligands (ketoH) (X = H for bpoH and X = CH_3O- for opoH) and (B)–(D) the α-diimines (enR): bipy (B), phen(C), dpamH(D) and H-atom labeling.

2.2. Instrumentation — physical measurements

Infrared (IR) spectra (400–4000 cm^{-1}) were recorded on a Nicolet FT-IR 6700 spectrometer with samples prepared as KBr pellets. UV–visible (UV–vis) spectra were recorded as Nujol mulls and in DMSO solutions at concentration in the range 10^{-5}–10^{-3} M on a Hitachi U-2001 dual beam spectrophotometer. ^1H NMR spectra were recorded at 300 MHz on a Bruker AVANCE^{III} 300 spectrometer using DMSO-d_6 as solvent. C, H and N elemental analyses were performed on a Perkin-Elmer 240B elemental microanalyzer. Molecular conductivity measurements were carried out with a Crison Basic 30 conductometer. Fluorescence spectra were recorded in solution on a Hitachi F-7000 fluorescence spectrophotometer. Viscosity experiments were carried out using an ALPHA L Fungilab rotational viscometer equipped with an 18 mL LCP spindle and the measurements were performed at 100 rpm. The simultaneous TG/DTG–DTA curves were recorded on a SETARAM thermal analyzer, model SETARAM SETSYS-1200. The samples of approximately 10 mg were heated in platinum crucibles, in a nitrogen atmosphere at a flow rate of 50 ml min^{-1}, within the temperature range 30–1000 °C, at a heating rate of 10 °C min^{-1}.

2.3. Synthesis of the complexes

2.3.1. Synthesis of $[Zn(keto)_2(H_2O)_2]$ (*1* and *5*)

Complexes **1** and **5** were synthesized according to our published procedure [44], by the addition of a methanolic solution (15 mL) of ketoH (1 mmol), deprotonated with CH_3ONa (1 mmol, 54 mg), to a methanolic solution (10 mL) of $Zn(NO_3)_2 \cdot 6H_2O$ (0.5 mmol, 148.75 mg) at room temperature. The reaction mixture was stirred for 2 h and then turned into yellowish. The solution was filtered and left for slow evaporation. After a few days a pale yellow microcrystalline product was collected with filtration, washed with cold water and air-dried.

$[Zn(opo)_2(H_2O)_2]$, ***1***: Yellow microcrystalline solid, yield 63%, 174 mg, conductivity in DMSO solution 3.1 μS/cm, analyzed as $[Zn(opo)_2(H_2O)_2]$, ($ZnC_{28}H_{26}O_8$), (MW = 555.5): C 60.48, H 4.68, Found: C 60.04, H 4.54. IR spectrum (KBr): selected peaks in cm^{-1}: 3439 (medium, (m)) ν(O–H) of coordinated water, 2816(m) ν(−OCH_3), 1612 (strong, (s)) and 1587(s) ν(C = O), 1363(s) ν(C–O → Zn), 603(m) ν(Zn–O); UV–vis: λ/nm (ε/M^{-1} cm^{-1}) as Nujol mull: 288.5, 321, 350; in DMSO: 288 (2400), 319 (1650), 347(sh (shoulder)) (1200). ^1H NMR spectrum in DMSO-d_6 (δ/ppm), 50 °C: 7.70–7.37 (12H, m, H^6, $H^{2'}$, $H^{3'}$, $H^{4'}$, $H^{5'}$and $H^{6'}$-opo), 6.60–6.45 (4H, br(broad), m, $H^3$and H^5-opo), and 3.84 (6H, s, CH_3O).

$[Zn(bpo)_2(H_2O)_2]$, ***5***: Yellow microcrystalline solid, yield 65%, 161 mg, conductivity in DMSO solution 2.4 μS/cm, analyzed as $[Zn(bpo)_2(H_2O)_2]$, ($ZnC_{26}H_{22}O_6$), (MW = 495.5): C 62.96, H 4.44, Found: C 62.55, H 4.24. IR spectrum (KBr): selected peaks in cm^{-1}: 3437 (medium, (m)) ν(O–H) of coordinated water, 2817(m) ν(−OCH_3), 1627 (strong, (s)) and 1601(s) ν(C = O), 1335(s) ν(C–O → Zn), 530(m) ν(Zn–O); UV–vis: λ/nm (ε/M^{-1} cm^{-1}) as Nujol mull: 265, 323, 395; in DMSO: 265 (6400), 320 (2300), 403 (sh) (350). ^1H NMR spectrum in DMSO-d_6 (δ/ppm): ^1H NMR spectrum in DMSO-d_6 (δ/ppm): 7.85–7.30 (14H, m, H^4, H^6, $H^{2'}$, $H^{3'}$, $H^{4'}$, $H^{5'}$and $H^{6'}$-bpo), and 7.05–6.87 (4H, br m, $H^3$and H^5-bpo).

2.3.2. Synthesis of $[Zn(keto)_2(enR)]$ (*2*–*4* and *6*–*8*)

A methanolic solution (10 mL) of bipy (1 mmol, 156 mg), phen (1 mmol, 180 mg) or dpamH (1 mmol, 171 mg) was added slowly to

a methanolic solution (10 mL) of [Zn(keto)$_2$(H$_2$O)$_2$] (**1** or **5**) (1 mmol) under stirring at room temperature. The reaction mixture was stirred for 2 h, reduced in volume and left for slow evaporation. The pale yellow microcrystalline product was filtered off and dried under vacuum.

[Zn(opo)$_2$(bipy)]·2CH$_3$OH, ***2****·2CH$_3$OH*: Yellow crystals, yield 65%, 240 mg, conductivity in DMSO solution 2.1 μS/cm, suitable for X-ray crystallography, analyzed as [Zn(opo)$_2$(bipy)]·2CH$_3$OH ($ZnC_{40}H_{38}N_2O_8$) (MW = 739.5): C 64.91, H 5.13, N 3.78; Found: C 64.73, H 5.07, N 3.75. IR spectrum (KBr): selected peaks in cm^{-1}: 3430(m) ν(O–H) of crystallized methanol, 1612(s) and 1587(s) ν(C = O), 1568(s) ν(C = N), 1542(s), 1364(s) ν(C–O → Zn), 840(m), 750(m) and 700(s) δ(C–H)$_{pyridyl}$, 586(m) ν(Zn–O), 472(weak, (w)) ν(Zn–N); UV–vis: λ/nm (ε/M^{-1} cm^{-1}) as Nujol mull: 290, 320, 363, 420; in DMSO: 288 (6100), 320 (5500), 365(sh) (850), 416 (530). ^{1}H NMR spectrum in DMSO-d$_6$ (δ/ppm): 7.67–7.30 (12H, m, H^6, H$^{2'}$, H$^{3'}$, H$^{4'}$, H$^{5'}$and H$^{6'}$-opo), 6.11(1H, s, H^3–opo), 5.95 (1H, d, *J* = 7.6 Hz, H^5-opo), 3.70 (6H, s, CH$_3$O), and 8.71 (2H, d, *J* = 3.8 Hz, H^3- and H$^{3'}$-bipy), 8.51 (2H, d, *J* = 7.8 Hz, H^6- and H$^{6'}$-bipy), 8.08 (2H, t, *J* = 7.8 Hz, H^5- and H$^{5'}$-bipy), and 7.04 (2H, br d, *J* = 7.8 Hz, H^4- and H$^{4'}$-bipy).

[Zn(opo)$_2$(phen)]·1CH$_3$OH, ***3****·1CH$_3$OH*: Pale yellow microcrystalline solid, yield 66%, 241 mg, conductivity in DMSO solution 1.8 μS/cm, analyzed as [Zn(opo)$_2$(phen)]·CH$_3$OH ($ZnC_{41}H_{34}N_2O_7$) (MW = 731.5): C 67.25, H 4.64, N 3.82; Found: C 67.02, H 4.57, N 3.70. IR spectrum (KBr): selected peaks in cm^{-1}: 3427(m) ν(O–H) of crystallized methanol,1612(s) ν(C = O), 1567(s) ν(C = N), 1360(m) ν(C–O → Zn), 840(m), 751(m) and 726(s) δ(C–H)$_{pyridyl}$, 605(m) ν(Zn–O), 415(m) ν(Zn–N); UV–vis: λ/nm (ε/M^{-1} cm^{-1}) as Nujol mull: 290, 325, 385; in DMSO: 284 (5500), 320 (2100), 385(sh) (420). ^{1}H NMR spectrum in DMSO-d$_6$ (δ/ppm), 50 °C: 9.06 (2H, br, H^2- and H^9-phen), 8.62 (2H, d, *J* = 6.3 Hz, H^4- and H^7-phen), 8.09 (2H, s, H^5- and H^6-phen), 7.89 (2H, br, H^3- and H^8-phen), 7.63–7.22 (12H, m, H^6, H$^{2'}$, H$^{3'}$, H$^{4'}$, H$^{5'}$and H$^{6'}$-opo), 6.49–6.22 (4H, br m, H^3 and H^5-opo), and 3.39 (6H, s, CH$_3$O).

[Zn(opo)$_2$(dpamH)], ***4***: Yellow microcrystalline solid, yield 68%,221 mg, conductivity in DMSO solution 0.8 μS/cm, analyzed as [Zn(opo)$_2$(dpamH)], ($ZnC_{38}H_{31}N_3O_6$) (MW = 690.5): C 66.04, H 4.49, N 6.08; Found: C 65.73, H 4.47, N 6.01. IR spectrum (KBr): selected peaks in cm^{-1}: 3317(m), 3192(m) and 3072(m) ν(N–H)$_{dpamH}$, 1643(s) δ(N–H)$_{dpamH}$, 1597 m ν(C = O), 1580(s) ν(C = N), 1359(s) ν(C–O → Zn), 842(m) and 768(s) δ(C–H)$_{pyridyl}$, 599(m) and 536(m) ν(Zn–O), 498(w) ν(Zn–N); UV–vis: λ/nm (ε/M^{-1} cm^{-1}) as Nujol mull: 289, 320, 355, 395; in DMSO: 287 (3200), 318 (3300), 353(sh) (350), 370(sh) (750). ^{1}H NMR spectrum in DMSO-d$_6$ (δ/ppm), 50 °C: 9.20 (1H, br s, H^7-dpamH), 8.22 (2H, br, H^3- and H$^{3'}$-dpamH), 7.88–7.47 (16H, m, H^6, H$^{2'}$, H$^{3'}$, H$^{4'}$, H$^{5'}$, H$^{6'}$-opo and H^5, H^5,H^6, H$^{6'}$-dpamH), 6.86 (2H, br m, H^4- and H$^{4'}$-dpamH). 6.62–6.45 (4H, br m, H^{3}and H^5-opo), and 3.85 (6H, s, CH$_3$O).

[Zn(bpo)$_2$(bipy)]·2CH$_3$OH, ***6****·2CH$_3$OH*: Yellow crystals, yield 60%, 203 mg, conductivity in DMSO solution 1.4 μS/cm, suitable for X-ray crystallography, analyzed as [Zn(bpo)$_2$(bipy)]·2CH$_3$OH, ($ZnC_{38}H_{34}N_2O_6$) (MW = 679.5): C 67.11, H 5.00, N 4.12; Found: C 66.73, H 4.98, N 4.10. IR spectrum (KBr): selected peaks in cm^{-1}: 3430(m) ν(O–H) of crystallized methanol, 1613(s) ν(C = O), 1570(s) ν(C = N), 1354(m) ν(C–O → Zn), 840(m), 762(s) and 704(s) δ(C–H)$_{pyridyl}$; 587(m) and 505(m) ν(Zn–O), 422(weak, (w)) ν(Zn–N); UV–vis: λ/nm (ε/M^{-1} cm^{-1}) as Nujol mull: 268, 323, 390; in DMSO: 271 (6300), 320 (3700), 380 (1200). ^{1}H NMR spectrum in DMSO-d$_6$ (δ/ppm), 50 °C: 8.69 (2H, br, H^3- and H$^{3'}$-bipy), 8.38 (2H, d, *J* = 7.4 Hz, H^6- and H$^{6'}$-bipy), 7.93 (2H, t, *J* = 7.4 Hz, H^5- and H$^{5'}$-bipy), 7.68–7.36 (16H, m, H^4, H^6, H$^{2'}$, H$^{3'}$, H$^{4'}$, H$^{5'}$, H$^{6'}$-bpo and H^4, H$^{4'}$-bipy), and 7.06–6.89 (4H, br m, H^{3}and H^5-bpo).

[Zn(bpo)$_2$(phen)], ***7***: Yellow microcrystalline solid, yield 66%, 211 mg, conductivity in DMSO solution 2.2 μS/cm, analyzed as [Zn(bpo)$_2$(phen)], ($ZnC_{38}H_{26}N_2O_4$) (MW = 639.5): C 71.30, H 4.06, N 4.38; Found: C 71.07, H 4.05, N 4.35. IR spectrum (KBr): selected peaks in cm^{-1}: IR spectrum (KBr): selected peaks in cm^{-1}: 1615(s) ν(C = O), 1573(s) ν(C = N), 1352(m) ν(C–O → Zn), 836(m), 780(m) and 724(s) δ(C–H)$_{pyridyl}$, 593(m) and 507(m) ν(Zn–O), 415(m) ν(Zn–N); UV–vis: λ/nm (ε/M^{-1} cm^{-1}) as Nujol mull: 275, 328, 400; in DMSO: 275 (7300), 325 (2700), 393 (1500). ^{1}H^{1}H NMR spectrum in DMSO-d$_6$ (δ/ppm), 50 °C: 9.09 (2H, br, H^2- and H^9-phen), 8.50 (2H, br, H^4- and H^7-phen), 8.03 (2H, s, H^5- and H^6-phen), 7.81 (2H, br, H^3- and H^8-phen), 7.71–7.28 (14H, m, H^4, H^6, H$^{2'}$, H$^{3'}$, H$^{4'}$, H$^{5'}$and H$^{6'}$-bpo), and 7.02–6.75 (4H, br m, H^{3}and H^5-bpo).

[Zn(bpo)$_2$(dpamH)], ***8***: Yellow microcrystalline solid, yield 63%, 204 mg, conductivity in DMSO solution 1.0 μS/cm, analyzed as [Zn(bpo)$_2$(dpamH)], ($ZnC_{36}H_{27}N_3O_4$) (MW = 630.5): C 68.52, H 4.28, N 6.66; Found: C 68.19, H 4.27, N 6.61. IR spectrum (KBr): selected peaks in cm^{-1}: 3303(m), 3192(m) and 3075(m) ν(N–H)$_{dpamH}$, 1643(s) δ(N–H)$_{dpamH}$, 1603(s) ν(C = O), 1573(s) ν(C = N), 1344(s) ν(C–O → Zn), 874(m), 827(m) and 760(s), 700(s) δ(C–H)$_{pyridyl}$, 593(m) and 517(m) ν(Zn–O), 498(w) ν(Zn–N); UV–vis: λ/nm (ε/M^{-1} cm^{-1}) as nujol mull: 268, 317, 420; in DMSO: 268 (4970), 316 (3700). 359(sh) (800), 370(sh) (300). ^{1}H NMR spectrum in DMSO-d$_6$ (δ/ppm): 9.58 (1H, br s, H^7-dpamH), 8.22 (2H, d, *J* = 4.2 Hz, H^3- and H$^{3'}$-dpamH), 7.82–7.33 (18H, m, H^4, H^6, H$^{2'}$, H$^{3'}$, H$^{4'}$, H$^{5'}$, H$^{6'}$-bpo and H^5, H$^{5'}$,H$^{6'}$-dpamH), and 7.06–6.83 (6H, m, H^3, H^5-bpo and H^4, H$^{4'}$-dpamH).

2.4. X-ray crystal structure determination

Slow crystallization from the reaction mixture in methanol yielded yellow crystals of compounds [Zn(opo)$_2$(bipy)].2CH$_3$OH (**2** · 2CH$_3$OH) and [Zn(bpo)$_2$(bipy)]. 2CH$_3$OH (**6** · 2CH$_3$OH). The diffraction data for single crystals were collected at 100 K with an Oxford Diffraction Xcalibur E diffractometer using Mo Kα radiation for compound **2** · 2CH$_3$OH, and at 130 K with an Oxford Diffraction SuperNova diffractometer using Cu Kα radiation for compound **6** · 2CH$_3$OH. The intensity data were collected and processed using CrysAlisPro software [45]. The structures were solved by direct methods with the program SIR-2004 [46] and refined by full-matrix least-squares method on F^2 with SHELXL-97 [47]. The carbon-bound hydrogen atoms were refined as riding on their carriers and their displacement parameters were set equal to 1.5U$_{eq}$(C) for the methyl groups and 1.2U$_{eq}$(C) for the remaining H atoms. The O–H group hydrogen atoms were located in electron density difference maps and freely refined. Crystallographic data, data collection and refinement details are given in Table 1. Molecular graphics were generated with ORTEP-3 for Windows [48] and Mercury 3.0 software [49].

2.5. DNA-binding studies

In order to study the interaction of DNA with the compounds, they were initially dissolved in DMSO (1 mM). Mixing of such solutions with the aqueous buffer solutions used in the studies never exceeded 5% DMSO (v/v) in the final solution, which was needed due to low aqueous solubility of some of the complexes and ketoH. All studies were performed at room temperature.

2.5.1. DNA-binding studied by UV-absorption spectroscopy

The interaction of the substituted 2-hydroxyphenones (opoH and bpoH) and complexes **1**–**8** with CT DNA has been studied by UV spectroscopy in order to investigate the possible binding modes to CT DNA and to calculate the binding constants to CT DNA (K$_b$). The UV spectra of CT DNA in the presence of each compound have been recorded for a constant CT DNA concentration in diverse mixing ratios (r = [compound]/[CT DNA]). The binding constants of the compounds with CT DNA, K$_b$, have been determined using the UV spectra of the complexes recorded for a constant concentration in the absence or presence of CT DNA for diverse r values. Control experiments with 5% DMSO were performed and no changes in the spectra of CT DNA were observed.

Table 1
Crystallographic data, data collection and refinement details for compounds **2** · $2CH_3OH$ and **6** · $2CH_3OH$.

	2 · $2CH_3OH$	**6** · $2CH_3OH$
Empirical formula	$[Zn(opo)_2(bipy)]\cdot 2CH_3OH$	$[Zn(bpo)_2(bipy)]\cdot 2CH_3OH$
CCDC no.	CCDC 970394	CCDC 970395
Formula weight	740.09	680.04
Crystal system	monoclinic	monoclinic
Temperature	100 K	130 K
Radiation	Mo Kα	Cu Kα
Space group	$P2_1/n$	$P2_1/n$
Unit cell dimensions	$a = 9.4803(1)$ Å	$a = 9.5980(1)$Å
	$b = 33.9218(4)$ Å	$b = 33.6995(4)$ Å
	$c = 11.1930(1)$ Å	$c = 10.0969(1)$ Å
	$\alpha = 90°$	$\alpha = 90°$
	$\beta = 90.668(1)°$	$\beta = 93.945(1)°$
	$\gamma = 90°$	$\gamma = 90°$
Volume	3599.30(7) $Å^3$	3258.08(6) Å3
Z, Z′	4, 1	4, 1
Absorption coefficient	0.738 mm^{-1}	1.461 mm^{-1}
Independent reflections/ R_{int}	6837/0.0399	6702/0.0199
Parameters/restraints	471/0	434/0
GOF	1.227	1.039
Final R indices: R2/wR2 (all data)	0.0449/0.0826	0.0348/0.0858
R1/wR1 (for $I > 2\sigma(I)$)	0.0408/0.0812	0.0314/0.0831
Largest difference peak/ hole (e $Å^{-3}$)	0.30/−0.39	0.40/−0.45

2.5.2. DNA-binding studied by viscosity measurements

The viscosity of a DNA solution (0.1 mM) has been measured at room temperature in the presence of increasing amounts of the compounds (substituted 2-hydroxyphenones or complexes **1**–**8**) up to *r* value of 0.35. The obtained data are presented as $(\eta/\eta_0)^{1/3}$ versus *r*, where η is the viscosity of DNA in the presence of compound, and η_0 is the viscosity of DNA alone in buffer solution.

2.5.3. Competitive studies with EB by fluorescence emission spectroscopy

The competitive studies of each compound with EB have been investigated by fluorescence emission spectroscopy in order to examine whether it is able to displace EB from its CT DNA–EB complex. The CT DNA–EB complex was prepared by adding 20 μM EB and 26 μM CT DNA in buffer (150 mM NaCl and 15 mM trisodium citrate at pH 7.0). The intercalating effect of the substituted 2-hydroxyphenones and complexes **1**–**8** with the DNA–EB complex was studied by adding a certain amount of a solution of the compound step by step into the solution of the DNA–EB complex. The influence of the addition of each compound to the DNA–EB complex solution has been obtained by recording the variation of fluorescence emission spectra with excitation wavelength $\lambda_{ex} = 540$ nm.

3. Results and discussion

3.1. Synthesis-general considerations of the complexes

The reaction of $Zn(NO_3)_2\cdot 6H_2O$ with two 2-hydroxyphenones (ketoH) in methanol (deprotonated by sodium methoxide) afforded solid microcrystalline compounds in good yield, according to reaction (1).

$$Zn(NO_3)_2.6H_2O + 2ketoH + 2CH_3ONa \rightarrow [Zn(keto)_2(H_2O)_2] + 2CH_3OH + 2NaNO_3 + 4H_2O. \quad (1)$$

The obtained zinc(II) complexes are neutral (conductivities in DMSO solutions were found in the range 0.8–3.1 μS cm^{-1}), and possess 1:2 metal-to-ligand composition, as it is indicated from elemental analyses. The complexes are formulated as $[Zn(keto)_2(H_2O)_2]$ (ketoH = opoH and bpoH, complexes **1** and **5**, respectively), and are soluble in MeOH, CH_3CN, CH_3COCH_3, CH_2Cl_2, DMF, DMSO but not in H_2O and Et_2O. The reaction of a methanolic solution of $[Zn(keto)_2(H_2O)_2]$ with equivalent amount of an enR led to the preparation of the mixed-ligand zinc complexes, $[Zn(keto)_2(enR)]$ (enR = bipy, phen and dpamH), (complexes **2**–**4** and **6**–**8**), according to reaction (2).

$$[Zn(keto)_2(H_2O)_2] + enR \rightarrow [Zn(keto)_2(enR)] + 2H_2O. \quad (2)$$

The complexes $[Zn(keto)_2(enR)]$ are soluble in DMF, DMSO, partially soluble in most organic solvents, but insoluble in H_2O and Et_2O. Evidence of the coordination mode of the ligands in the new zinc compounds is also arisen from the interpretation of the IR, UV–vis and ^1H NMR data of the 2-hydroxy-benzophenone ligands and the complexes. In these complexes, the 2-hydroxy-benzophenones behave as bidentate monoanionic ligands, coordinated through the carbonyl and the phenolate oxygen atoms, while the enR as bidentate neutral ligand completing the octahedral geometry around zinc. The structure for the compounds **2** and **6** was verified by single-crystal X-ray diffraction analysis.

3.2. Spectroscopy (IR, UV–vis and ^1H NMR)

IR spectroscopy has been used in order to confirm the deprotonation and binding mode of 2-hydroxybenzophenones. In the spectra of the free ketoH the intense bands of the stretching and bending vibrational modes of the phenolic OH around 3200 cm^{-1} and 1410 cm^{-1}, respectively, disappear from the spectra of all complexes indicating the ligand deprotonation [50,51]. Also, the bands originating from the C–O stretching vibrations at 1245–1285 cm^{-1} exhibit positive shifts towards 1350–1380 cm^{-1} in the complexes, denoting coordination through the carbonyl oxygen of the ligand. The band at ~1660 cm^{-1} attributable to the carbonyl bond ν(R − C = O) of the free ligand, upon coordination is shifted to lower frequency ~1605 cm^{-1}, thus denoting its bidentate mono-anionic character [52,53]. Also, the intense bands at ~1580 cm^{-1}, attributable to the stretching vibration of *ν*(C═N (aromatic bond)) are present in the mixed-ligand complexes, denoting the coordination through the nitrogen atoms of the α-diimine ligand. The medium-to-low intensity bands at 530–560 cm^{-1} and 415–470 cm^{-1} are attributed to the coordination bonds (Zn–O and Zn–N, respectively) according to the literature [51].

The ultraviolet–visible (UV–vis) spectra of the complexes have been recorded as Nujol mull and in DMSO solution and are similar, suggesting that the complexes retain their structure in solution. In addition, in order to explore the stability of complexes in buffer solution, the UV–vis spectra in the series of pH (pH range 6–8, since the biological experiments are performed at pH = 7) with the use of diverse buffer solutions (150 mM NaCl and 15 mM trisodium citrate at pH values regulated by HCl solution) have also been recorded. Significant changes (shift of the λ_{max} or new peaks) have not been observed in the spectra, indicating that complexes **1**–**8** keep their integrity in the pH range 6–8 [54,55].

^1H NMR spectroscopy has also been used in order to confirm the deprotonation of the 2-hydroxybenzophenones and the stability of the complexes in solution. The deprotonation of the phenolic hydrogen can be easily seen from the absence of the −OH signal, which is obvious to the ^1H NMR spectra of the free ligand, appearing as single peak at δ = 12 ppm for opoH (Fig. S1) and at 10.54 ppm for bpoH. The ^1H NMR spectra are consistent with the obtained structures of **1**–**8**. It should be mentioned that most spectra were taken at 50 °C because of the dynamic line broadening of the peaks due to exchange processes. All the expected sets of signals related to the presence of the ligands in the corresponding compounds are present and they are slightly shifted as expected upon binding to zinc ion. The ^1H NMR spectra of the complexes give signals attributable to the protons of the benzene ring at δ = 7.85–6.45 ppm. The absence of additional set of signals related to dissociated ligands suggests that all complexes remain intact in solution [56,57] (Fig. 1). Similar results have been referred for the Schiff base

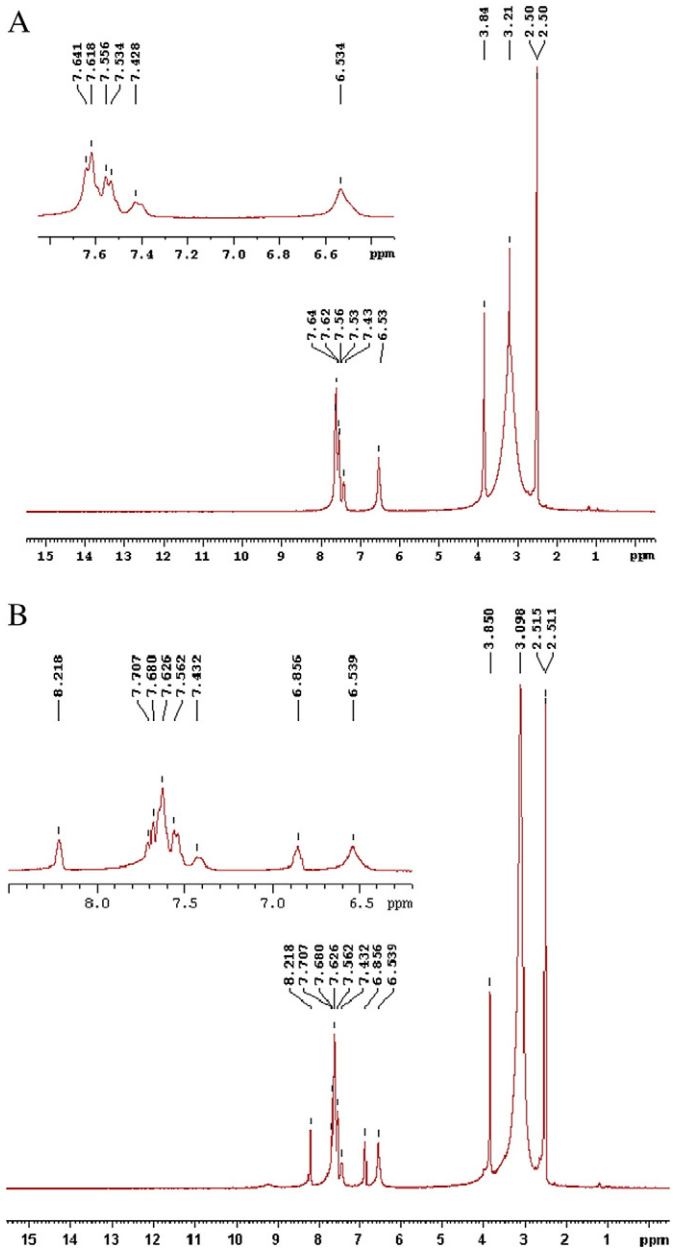

Fig. 1. ^{1}H NMR spectra of (A) $[Zn(opo)_2(H_2O)_2]$ **1** and (B) of $[Zn(opo)_2(dpamH)]$ **4** in d_6-DMSO.

ligand 2-hydroxy-3-methoxybenzaldehyde semicarbazone and its complexes [58].

The fact that the complexes are non-electrolytes in DMSO solution ($\Lambda_M \leq 3.0$ μS/cm, in 1 mM DMSO solution), they have the same UV–vis spectral pattern in Nujol, in DMSO solution and in the presence of the buffer solution and their ^{1}H NMR spectra confirm no dissociation, suggests that the compounds are stable and keep their integrity in solution [55,59].

3.3. Description of the structures

The complexes of the formula $[Zn(keto)_2(enR)]$ can exist as three geometric isomers I–III (Scheme 2) that can have similar but not identical properties. All three isomeric molecules are chiral, with isomers I and II exhibiting C_2 symmetry and isomer III being asymmetric. In case of complexes **2** and **6**, X-ray crystallography has been applied to determine the isomeric form of the isolated compound.

The molecular structures of $[Zn(opo)_2(bipy)]\cdot 2CH_3OH$ (**2** · $2CH_3OH$) and $[Zn(bpo)_2(bipy)]\cdot 2CH_3OH$ (**6** · $2CH_3OH$) with the atom numbering scheme are shown in Fig. 2 and selected bond distances and angles are given in Table 2. The complexes crystallize as racemic compounds and the asymmetric part of the unit cell contains one neutral complex molecule and two methanol molecules linked to the phenolate oxygen atoms via O–H···O hydrogen bonds. The zinc(II) cation is in a distorted octahedral environment formed by two nitrogen atoms from the bipy ligand and four oxygen atoms from the two keto ligands. The $Zn–O_{phenolate}$ bond lengths (2.015, 2.020 Å in **2** and 2.026, 2.049 Å in **6**) are significantly shorter than the corresponding $Zn–O_{carbonyl}$ bonds (2.148, 2.164 Å in **2** and 2.106, 2.130 Å in **6**). In both crystals, the molecules have an approximate C_2 symmetry. The arrangement of the deprotonated 2-hydroxybenzophenone ligands around the metal center is such that their phenolate oxygen atoms coordinate *trans* to the bipy N atoms and thus both isolated compounds represent the isomer II. The six-membered chelate rings formed by the keto ligands are strongly nonplanar which allows for intramolecular π–π stacking interactions of their phenolate fragments. The two stacked aromatic rings are inclined by 12.9 and 11.9° and their centroids are 3.934 and 3.974 Å apart in **2** and **6**, respectively. As intramolecular stacking interactions can be solely formed in isomer II, they are the most probable reason for the stability and preferred formation of isomer II of **2** and **6**.

The crystal packing of **2** · $2CH_3OH$ is to a large extent determined by π–π stacking interactions between the bipy ligands that organize the molecules into infinite stacking extending along the a axis, with the distances between the centroids of the stacked pyridine rings ranging from 3.755 to 3.826 Å (Fig. 3). This stacking is additionally strengthened by C–H···O interactions (H···O 2.32 Å) between one of the bipy H atoms and the phenolate oxygen. In **6** · $2CH_3OH$, the stacking interactions are not so pronounced and occur only between a pair of pyridine rings, with their centroids at a distance of 3.613 Å. Instead, a short contact of 2.63 Å is formed between one C–H group of the methanol molecule and the centroid of the pyridine rings not involved in stacking interactions (Fig. 3).

3.4. Thermal studies

The thermal behavior for five compounds (**1**, **5**, **3**, **7** and **8**) was studied in nitrogen atmosphere and in the temperature range ambient to 980 °C

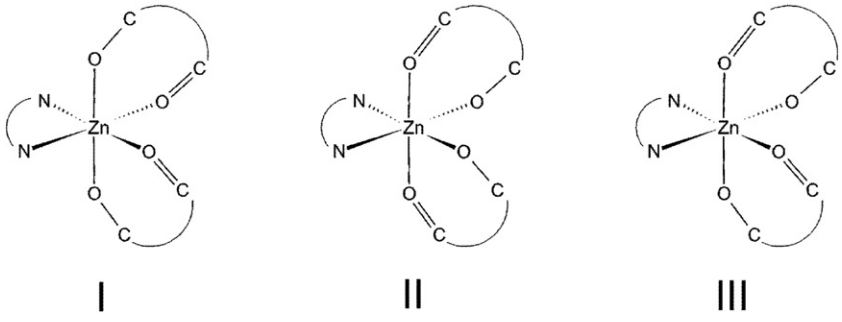

Scheme 2. Geometric isomers (I–III) of the molecules $[Zn(keto)_2(enR)]$.

by using the simultaneous TG/DTG–DTA technique. The temperature ranges, the determined percentage mass losses, and the thermal effects accompanying the decomposition are given in Table S1. Representative thermal curves are depicted for the complexes $[Zn(bpo)_2(H_2O)_2]$ **5** and $[Zn(bpo)_2(dpamH)]$ **8** in Fig. 4. For complexes **1** and **5** (absence of enR ligand), the decomposition takes place without melting, as it is evidence from the DTA curves (Fig. 4(A) for complex **5**), while the first mass loss coincides with the elimination of the two coordinated water molecules. Upon further heating, the elimination of the 2-hydroxybenzophenone ligand takes place, as a whole molecule or in fragments (Table S1), leading to a carbonaceous ZnO. The complex nature of thermal decomposition for analogous transition metal complexes has also recently been referred [34,44,60], while the kind of carbonaceous residue (ZnO and un-pyrolized compounds as organic part) has been observed in analogous zinc complexes with the Schiff base 5-bromosalicylaldehyde isonicotinoylhydrazone [61].

The thermal decomposition of the complexes in the presence of enR ligands (**3**, **7** and **8**) is even more complicated. The decomposition happens after the melting of the complexes, evidence arising from the sharp endothermic DTA peaks (Fig. 4(B) for **8**). The melting points of the studied compounds (~210–230 °C) were also determined by automated melting point capillary tube system in static air, confirming the melting points found on the DTA curves. Upon further heating, the decomposition continues with the elimination of the ketone fragments with sudden mass loss in two stages, while in the third stage the gradually mass loss of the enR ligand takes place in the temperature range 400–980 °C, leading to the metal oxide, ZnO.

3.5. Interaction of the compounds with calf-thymus DNA

Covalent and/or non-covalent interactions are the most usual binding modes of transition metal complexes to DNA. Non-covalent interactions to DNA include the intercalation of the complex within DNA helix via the existence of π → π stacking interaction between the complex and DNA nucleobases, minor- or major-groove binding via the formation of van der Waals forces or hydrogen-bonding or hydrophobic bonding along minor or major groove of DNA helix and electrostatic interactions upon the appearance of Coulomb forces between cationic metal complexes and the negatively-charged phosphate groups of DNA. The covalent binding exists when one at least labile ligand of the complex is replaced by a nitrogen base of DNA such as guanine N7 [62]. The DNA-interaction studies of the two substituted phenones (opoH and bpoH) and their complexes **1**–**8** are of special significance since a thorough research of the literature has not revealed any relevant studies concerning the ketoHs used herein or any of their complexes.

3.5.1. DNA-binding study with UV spectroscopy

The interaction of the compounds with CT DNA is usually monitored by UV spectroscopy since the changes observed in the UV spectra upon titration may provide evidence of the existing interaction mode; a hypochromism due to π → π stacking interactions may appear in the case of the intercalative binding mode, while red-shift (bathochromism) may be observed when the DNA duplex is stabilized [63].

The UV spectra have been recorded for a constant CT DNA concentration at different [complex]:[DNA] mixing ratios (r) (up to 0.3). The UV spectra of CT DNA in the presence of opoH and its complexes **1**–**4** at diverse r values have not exhibited any significant change of the intensity of the DNA band at $\lambda_{max} = 258$ nm while a slight red-shift (<3 nm) of the λ_{max} up to 261 nm has been observed. For bpoH and its complexes **5**–**8**, a hyperchromism of the DNA accompanied by a 3-nm bathochromism band has been observed (UV spectra of a CT DNA solution in the presence of complex **6** are shown representatively in (Fig. S2)). The recorded behavior may be considered as an evidence of the formation of a new adduct of the compound with double-helical CT DNA which results in the stabilization of the CT DNA duplex [64].

In the UV region of the spectra of the free ketoHs or complexes **1**–**8**, the intense absorption bands observed in the spectra of the complexes can be attributed to the intraligand transition of the coordinated ligands [33,52,65,66]. The changes observed in the intraligand transitions bands of complexes **1**–**8** upon addition of CT DNA solution in diverse r values (up to $1/r = 2$) may reveal the existence of interaction between each complex and CT DNA and may give first indication of the possible mode of binding. UV spectra of a DMSO solution of complexes **2** and **6** in the presence of a CT DNA solution (up to $1/r = 2$) are shown representatively in Fig. 5.

In the UV spectrum of opoH and its complexes **1**–**4**, two intraligand bands appear in the UV region; band I at ~288 nm and band II at ~320 nm (Fig. 5(A)). Upon addition of increasing amounts of CT DNA these two bands exhibit a slight hypochromism up to 3% while no significant shift of the λ_{max} of these bands occurs (Table 3). For the bpo compounds, an intraligand band located in the region 315–325 nm has been observed as in Fig. 5(B). The addition of CT DNA to bpoH or complexes **5**–**8** results in a slight hypochromism (<3%) or hyperchromism (up to 10%) with no shift of the position of λ_{max} (Table 3).

The results derived from the UV titration experiments suggest that all compounds can bind to CT DNA [67], although no safe conclusions concerning the interaction mode of the compounds to CT DNA can be derived. As it is known, the exact mode of interaction with DNA cannot be concluded only by UV spectroscopic studies and more techniques should be combined in order to come to a safe conclusion. The magnitude of the binding strength a compound to CT DNA may be estimated

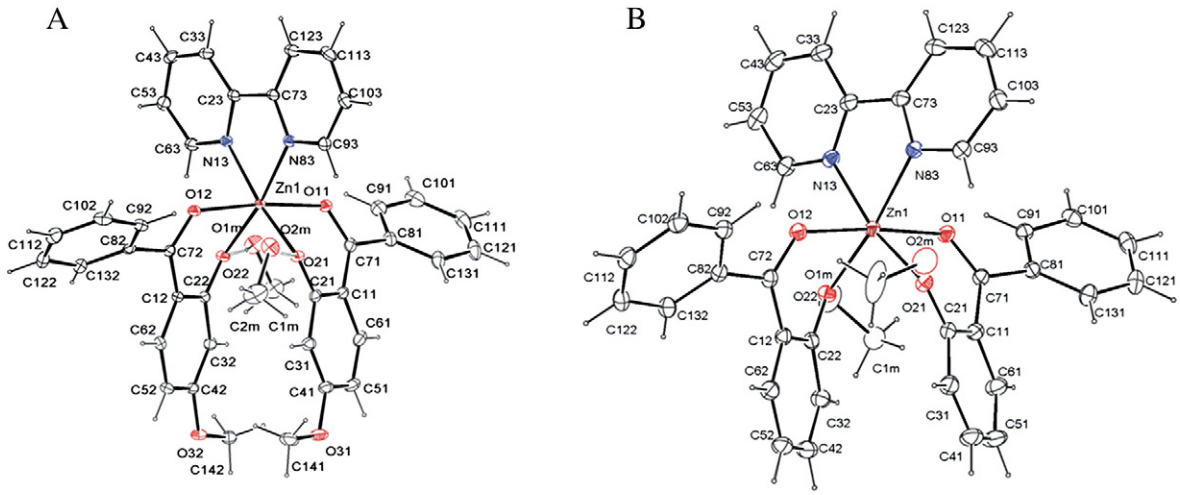

Fig. 2. The molecular structures of (A) **2** · $2CH_3OH$ and (B) **6** · $2CH_3OH$.

Table 2
Selected bond distances (Å) and angles (°) for complexes **2** · $2CH_3OH$ and **6** · $2CH_3OH$.

Bond distance	2 · $2CH_3OH$	6 · $2CH_3OH$
Zn(1)–O(11)	2.106(1)	2.164(1)
Zn(1)–O(21)	2.026(1)	2.020(1)
Zn(1)–O(12)	2.130(1)	2.148(1)
Zn(1)–O(22)	2.049(1)	2.015(1)
Zn(1)–N(13)	2.118(2)	2.144(1)
Zn(1)–N(83)	2.152(2)	2.142(1)
Bond angle	**2** · $2CH_3OH$	**6** · $2CH_3OH$
O(11)–Zn(1)–O(21)	83.46(6)	83.78(4)
O(11)–Zn(1)–O(12)	173.75(6)	175.05(4)
O(11)–Zn(1)–O(22)	93.18(6)	92.20(4)
O(11)–Zn(1)–N(13)	96.15(6)	91.84(4)
O(11)–Zn(1)–N(83)	90.74(6)	86.36(4)
O(21)–Zn(1)–O(12)	91.68(5)	93.97(4)
O(21)–Zn(1)–N(13)	171.03(6)	168.62(5)
O(21)–Zn(1)–O(22)	94.49(6)	97.23(4)
O(12)–Zn(1)–O(22)	83.25(5)	83.70(4)
O(12)–Zn(1)–N(13)	89.26(6)	91.17(4)
O(12)–Zn(1)–N(83)	93.54(6)	98.17(4)
O(22)–Zn(1)–N(13)	94.49(6)	93.43(5)
O(22)–Zn(1)–N(83)	170.91(6)	169.64(5)
N(13)–Zn(1)–N(83)	76.93(6)	76.38(5)
O(21)–Zn(1)–N(83)	94.10(6)	92.82(5)

through the calculation of the binding constant K_b, which can be obtained by monitoring the changes in the absorbance at the corresponding λ_{max} with increasing concentrations of CT DNA [64]. K_b is given by the ratio of slope to the y intercept in plots $\frac{[DNA]}{(\varepsilon_A-\varepsilon_f)}$ versus [DNA] (Figs. S3 and S4), according to Wolfe–Shimer Eq. (3) [68]:

$$\frac{[DNA]}{(\varepsilon_A-\varepsilon_f)}=\frac{[DNA]}{(\varepsilon_b-\varepsilon_f)}+\frac{1}{K_b(\varepsilon_b-\varepsilon_f)} \quad (3)$$

where [DNA] is the concentration of DNA in base pairs, $\varepsilon_A = A_{obsd}/[compound]$, ε_f = the extinction coefficient for the free compound and ε_b = the extinction coefficient for the compound in the fully bound form. The values of K_b for the two ketoHs and their complexes **1**–**8**, as calculated by Eq. (3) and the plots in Figs. S3 and S4, are given in Table 3.

The K_b values of the compounds are moderate to high suggesting their strong binding to CT DNA [65,66], with free opoH bearing the highest K_b value ($=5.20(\pm0.19)\times10^6\ M^{-1}$) of all compounds and complex **3** having the highest K_b value ($=4.89(\pm0.12)\times10^6\ M^{-1}$) among the complexes. Free opoH exhibits higher K_b value than its complexes **1**–**4**, while the bpo complexes **5**–**7** have higher K_b values than free bpoH. The K_b values of most compounds are similar or higher than that of the classical intercalator EB ($K_b = 1.23(\pm0.07)\times10^5\ M^{-1}$) [69], a fact that may be a first indication of the ability of the compounds to displace EB from the EB–DNA compound, in the case of intercalation.

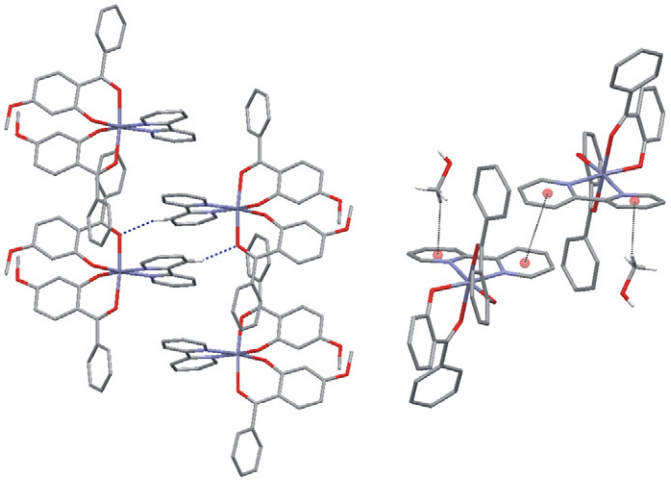

Fig. 3. The stacking formed by π–π interactions between bipy ligands in **2** · $2CH_3OH$ (left) and π–π and C–H···π interactions in **6** · $2CH_3OH$.

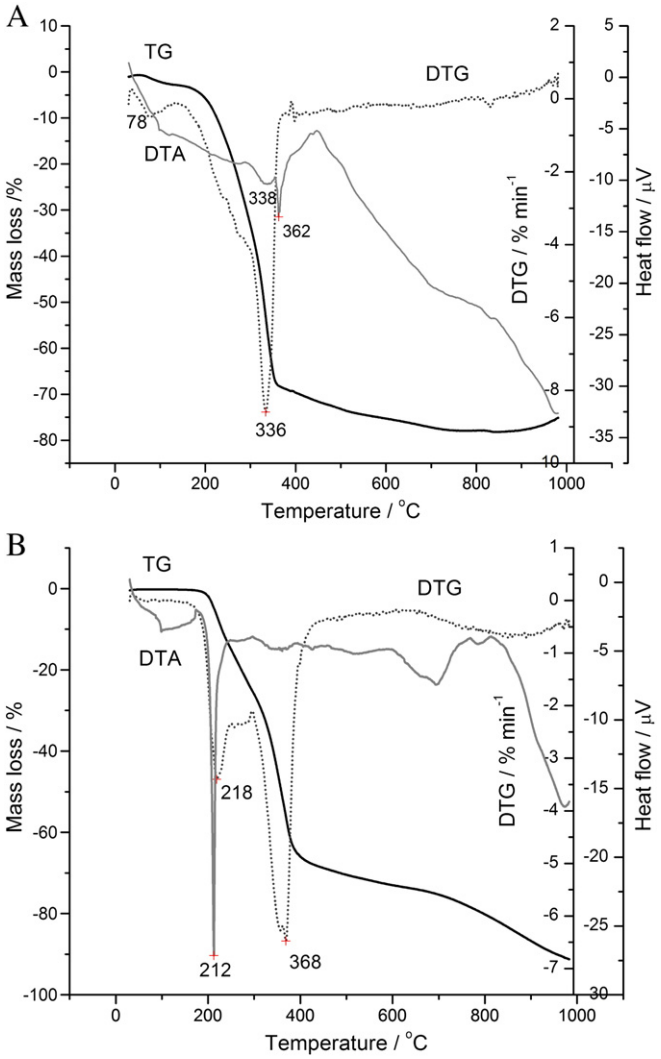

Fig. 4. Thermoanalytical curves (TG, DTG, DTA) for the complexes: (A) $[Zn(bpo)_2(H_2O)_2]$, **5** and (B) $[Zn(bpo)_2(dpamH)]$, **8**, with heating rate 10 °C min^{-1} in N_2 atm.

3.5.2. DNA-viscosity measurement in the presence of the compounds

The measurement of the DNA viscosity upon addition of a compound provides significant aid to clarify the interaction mode of a compound with DNA, since the viscosity of DNA is sensitive to DNA length changes. The relation between relative solution viscosity (η/η_0) and DNA length (L/L_0) is given by the Equation $L/L_0 = (\eta/\eta_0)^{1/3}$, where L_0 denotes the apparent molecular length in the absence of the compound [65,66].

The interaction of a compound to DNA grooves via a partial or non-classic intercalation (i.e. electrostatic interaction or external groove-binding) results in a bend or kink in the DNA helix and subsequently a slight shortening of its effective length may be provoked; in such a case, the DNA-viscosity may show a slight decrease or may remain unchanged. In the case of intercalative binding, the insertion of the compound in between the DNA base pairs results in an increase of the separation distance of base pairs being at the intercalation sites aiming

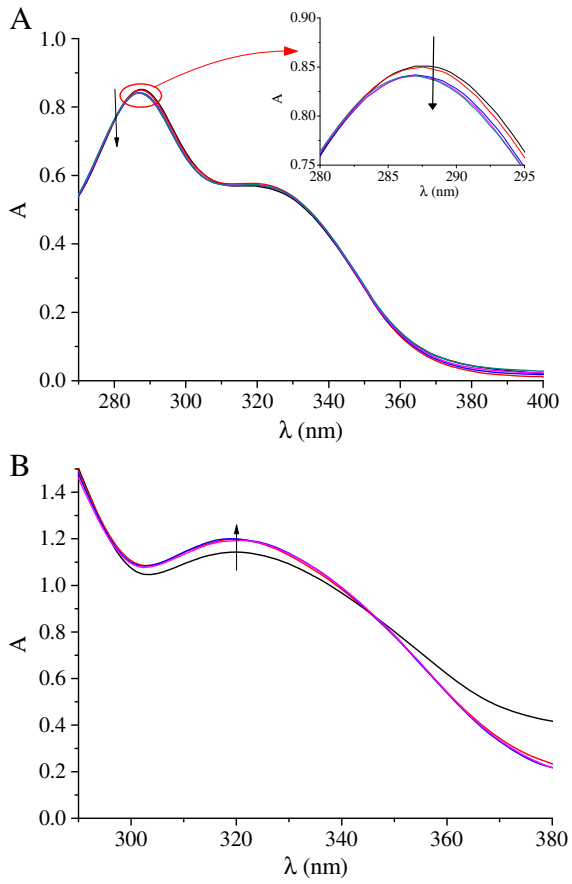

Fig. 5. UV spectra of a DMSO solution of complex (A) **2** (2.5×10^{-5} M) and (B) **6** (2×10^{-4} M) in the presence of CT DNA at increasing amounts (up to 1/r = 2). The arrows show the changes upon increasing amounts of CT DNA.

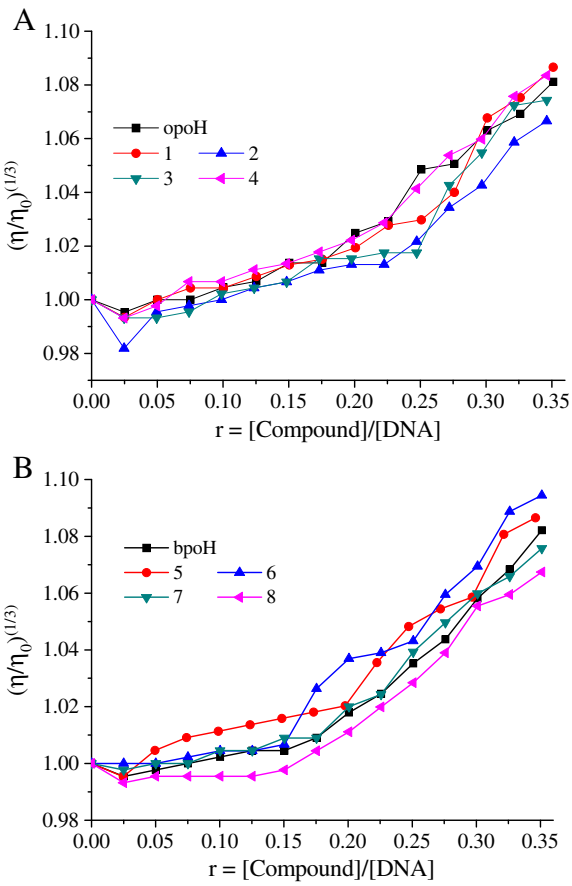

Fig. 6. Relative viscosity $(\eta/\eta_o)^{1/3}$ of CT DNA (0.1 mM) in buffer solution (150 mM NaCl and 15 mM trisodium citrate at pH 7.0) in the presence of (A) opoH and complexes **1**–**4** and (B) bpoH and complexes **5**–**8**, at increasing amounts (r = 0–0.35).

to host the bound compound; therefore, the increase of the length of the DNA helix if the reason of the DNA viscosity increase, the magnitude of which is usually in accordance to the strength of the interaction [33,59,65,66,70].

Viscosity measurements were carried out on CT DNA solutions (0.1 mM) upon addition of increasing amounts of the compounds (up to the value of r = 0.35) at room temperature (Fig. 6). The relative viscosity of DNA solution upon addition of all compounds seems to be stable up to r = 0.15–0.20 suggesting a partial or non-classic intercalation, while for r > 0.20 the DNA viscosity exhibits an increase suggesting the existence of intercalation; this increase is less pronounced than that observed in the recently reported Zn complexes with substituted salicylaldehydes as ligands [33].

In conclusion, the behavior of the DNA viscosity observed upon addition of the compounds is in accordance with the indications derived from UV spectroscopic studies, and albeit not so clear, it may be considered an evidence of the existence of an intercalative binding mode to DNA.

Table 3
Spectral features of the UV spectra of ketoH and complexes **1**–**8** upon addition of DNA (band studied in λ(nm), percentage of hyperchromism or hypochromism ΔA(%), and hypsochromism or bathochromism Δλ(nm)) and the DNA binding constants (K_b) of ketoH and complexes **1**–**8**.

Compound	λ(nm) (ΔA(%) [a], Δλ(nm)[b])	K_b (M^{-1})
opoH	288(−3, 0), 319(−2.5, 0)	$5.20(\pm0.19) \times 10^6$
$[Zn(opo)_2(H_2O)_2]$, **1**	288(−2.5, 0), 319(−0, 0)	$3.73(\pm0.20) \times 10^5$
$[Zn(opo)_2(bipy)]$, **2**	288(−1, 0), 320(−0, 0)	$6.45(\pm0.21) \times 10^5$
$[Zn(opo)_2(phen)]$, **3**	284(−2, +1), 320(+1.5, 0)	$4.89(\pm0.12) \times 10^6$
$[Zn(opo)_2(dpamH)]$, **4**	287(−1.5, 0), 318(−2.5, 0)	$1.96(\pm0.41) \times 10^5$
bpoH	319(−2.5, +1)	$9.58(\pm0.40) \times 10^4$
$[Zn(bpo)_2(H_2O)_2]$, **5**	320(+10, 0)	$3.42(\pm0.30) \times 10^5$
$[Zn(bpo)_2(bipy)]$, **6**	320(+4, 0)	$6.89(\pm0.12) \times 10^5$
$[Zn(bpo)_2(phen)]$, **7**	325(+5, 0)	$7.68(\pm0.16) \times 10^5$
$[Zn(bpo)_2(dpamH)]$, **8**	316(−3, 0)	$6.06(\pm0.22) \times 10^4$

[a] "+" denotes hyperchromism and"−"denotes hypochromism.
[b] "+" denotes red-shift and"−"denotes blue-shift.

3.5.3. Competitive studies with ethidium bromide

Ethidium bromide (EB = 3,8-diamino-5-ethyl-6-phenyl-phenanthridinium bromide) is a typical indicator of intercalation since it emits intense fluorescence in the presence of DNA due to the strong intercalation of the planar EB phenanthridine ring between adjacent base pairs on the double DNA helix [71]. Upon the addition of a compound which can bind via intercalation to DNA equally or more strongly than EB to a solution containing the EB–DNA complex, a quenching of the DNA-induced EB fluorescence emission may appear.

The two substituted 2-hydroxybenzophenones (opoH and bpoH) and their complexes **1**–**8** do not show any significant fluorescence at room temperature in solution or in the presence of CT DNA, when excited at 540 nm. The addition of these compounds to a solution containing EB does not provoke quenching of free EB fluorescence and no new peaks appear in the spectra. Therefore, the changes observed in the fluorescence emission spectra of a solution containing the EB–DNA complex upon addition of the compounds can be used to study the ability of the compounds to displace EB from the EB–DNA complex [72].

The emission spectra of EB bound to CT DNA in the absence and presence of each compound have been recorded for [EB] = 20 μM, [DNA] = 26 μM for increasing amounts of each compound up to the

value of r = 2.5, in some cases. The addition of the compounds at diverse *r* values results in a rather significant decrease of the intensity of the emission band (Fig. 7 and Table 4) of the EB–DNA system at 592 nm indicating the competition of the compounds with EB in binding to DNA. The observed quenching of EB–DNA fluorescence suggests that the compounds have moderate to significant ability to displace EB from the EB–DNA complex, thus probably interacting with CT DNA by the intercalative mode.

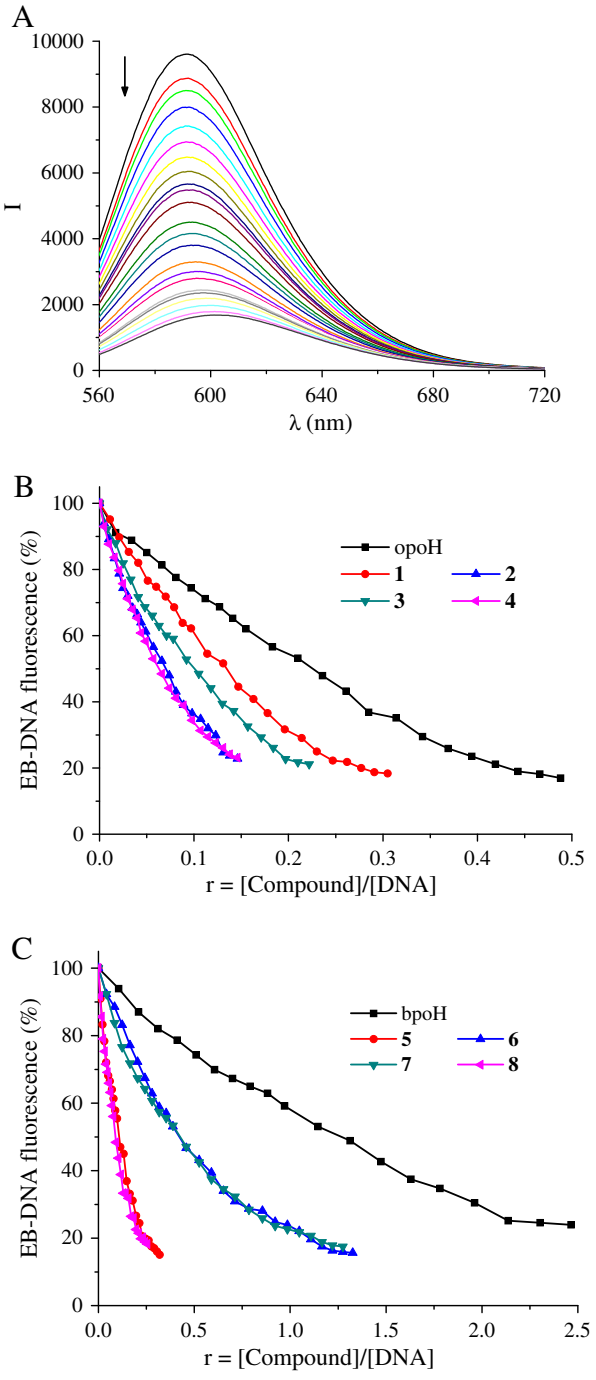

Fig. 7. (A) Fluorescence emission spectra (λ_{ex} = 540 nm) of a buffer solution (150 mM NaCl and 15 mM trisodium citrate at pH 7.0) containing EB–DNA in the presence of increasing amounts (up to r = 1.4) of complex **6**. (B) and (C) Plot of EB–DNA relative fluorescence emission intensity (%I/Io) at λ_{em} = 592 nm vs *r* (*r* = [compound]/[DNA]) in buffer solution (150 mM NaCl and 15 mM trisodium citrate at pH 7.0) in the presence of (B) opoH and complexes **1**–**4** (quenching up to 17% of the initial EB–DNA fluorescence for opoH, 18.5% for **1**, 23% for **2**, 21% for **3** and 23% for **4**) and (C) bpoH and complexes **5**–**8** (quenching up to 24% of the initial EB–DNA fluorescence for bpoH, 15% for **5**, 15.5% for **6**, 17.5% for **7** and 18.5% for **8**).

Table 4
Quenching of EB–DNA fluorescence (ΔI/Io, %) and Stern–Volmer constants (K_{SV}) for the ketoH and their complexes **1**–**8**.

Compound	EB–DNA fluorescence quenching (ΔI/Io, %)	Ksv (M^{-1})
opoH	83.0	$1.01(\pm0.05) \times 10^5$
$[Zn(opo)_2(H_2O)_2]$, **1**	81.5	$3.19(\pm0.17) \times 10^5$
$[Zn(opo)_2(bipy)]$, **2**	77.2	$4.02(\pm0.14) \times 10^5$
$[Zn(opo)_2(phen)]$, **3**	78.8	$2.82(\pm0.13) \times 10^5$
$[Zn(opo)_2(dpamH)]$, **4**	76.9	$4.90(\pm0.15) \times 10^5$
bpoH	76.0	$1.80(\pm0.08) \times 10^4$
$[Zn(bpo)_2(H_2O)_2]$, **5**	85.0	$3.83(\pm0.14) \times 10^5$
$[Zn(bpo)_2(bipy)]$, **6**	84.5	$7.63(\pm0.26) \times 10^4$
$[Zn(bpo)_2(phen)]$, **7**	82.5	$8.02(\pm0.22) \times 10^4$
$[Zn(bpo)_2(dpamH)]$, **8**	81.5	$3.95(\pm0.12) \times 10^5$

The Stern–Volmer constant, K_{SV} (in M^{-1}), may be used to evaluate the quenching ability of each compound [33,73] according to Eq. (4):

$$\frac{Io}{I} = 1 + K_{SV}[Q] \quad (4)$$

where Io and I are the emission intensities in the absence and the presence of the quencher, respectively, [Q] is the concentration of the quencher (the substituted 2-hydroxybenzophenones and their complexes **1**–**8**). K_{SV} is obtained by the slope of the diagram $\frac{Io}{I}$ vs [Q] in Stern–Volmer plots of DNA–EB (Figs. S5 and S6). The experimental data indicate that the quenching of EB bound to DNA provoked by the compounds is in good agreement (R ≥ 0.99) with the linear Stern–Volmer equation (Eq. (4)). The Stern–Volmer constants, K_{SV}, of the compounds are moderate to high (Table 4) showing that they can displace EB and bind relatively tightly to DNA [33,73,74]. Additionally, the opo compounds present higher Ksv than the bpo compounds, a feature present in the calculated K_b values from UV spectroscopic studies.

4. Conclusions

The synthesis and characterization of mononuclear zinc complexes with 2-hydroxybenzophenones (ketoH), (2-hydroxybenzophenone = bpoH and 4-methoxy-2-hydroxybenzophenone = opoH) in the absence $[Zn(keto)_2(H_2O)_2]$, or presence of a N,N′-donor heterocyclic ligand (enR) such as bipy, phen or dpamH, $[Zn(keto)_2(enR)]$, have been synthesized and characterized by IR, UV and ^{1}H NMR spectroscopies. The 2-hydroxybenzophenones are chelated to the metal ion through the phenolate and one carbonyl oxygen atoms. The crystal structures of $[Zn(opo)_2(bipy)]\cdot2MeOH$ ***2***·2MeOH and $[Zn(bpo)_2(bipy)]\cdot2MeOH$ ***6***·2MeOH have been determined by X-ray crystallography revealing a six-coordinated Zn(II) in a distorted octahedral environment. The thermal stability of the zinc complexes has been investigated by simultaneous TG/DTG–DTA technique. The stable in air complexes at room temperature are decomposed at higher temperatures leading to the pure metal oxide ZnO or to a mixture of ZnO plus un-pyrolized carbon.

UV spectroscopic studies have revealed the ability of the substituted 2-hydroxybenzophenones and their complexes to bind to CT DNA with complex **3** having the highest K_b value ($=4.89(\pm0.12) \times 10^6$ M^{-1}) among the complexes and free opoH exhibiting the highest K_b value ($=5.20(\pm0.19) \times 10^6$ M^{-1}) among the compounds examined, which are higher than the K_b value of EB. DNA viscosity measurements have revealed an intercalative binding mode of most compounds to CT DNA. Competitive binding studies with EB have shown a moderate to significant ability of the compounds to displace the typical intercalator EB from the EB–CT DNA complex, suggesting their competition with EB for the intercalation site of DNA. In general, the opo compounds may be considered as better DNA-binders and EB-displacing compounds that the bpo compounds, since they present higher K_b and K_{sv}

values than the bpo corresponding compounds. The existing results of the reported substituted 2-hydroxybenzophenones and their complexes as DNA intercalators are the first ever reported and are promising revealing a new possibility for their use as potential metallodrugs.

Abbreviations

Bipy	2,2′-bipyridine
bpoH	2-hydroxy-benzophenone
CT	calf–thymus
DMF	N,N-dimethylformamide
dpamH	2,2′-dipyridylamine
EB	ethidium bromide, 3,8-diamino-5-ethyl-6-phenyl-phenanthridinium bromide
enR	N,N′-donor heterocyclic ligand
ketoH	substituted 2-hydroxybenzophenones
m	medium
opoH	2-hydroxy-4-methoxy-benzophenone
phen	1,10-phenanthroline
s	strong
sh	shoulder
w	weak

Appendix A. Supplementary data

The crystal structures of compounds **2** and **6** have been submitted to the CCDC and have been allocated the deposition numbers CCDC 970394 and 970395, respectively. These data can be obtained free of charge via www.ccdc.cam.ac.uk/conts/retrieving.html (or from the Cambridge Crystallographic Data Centre, 12 Union Road, Cambridge CB21EZ, UK; fax: (+44) 1223-336-033; or deposit@ccdc.cam.ac.uk). Supplementary data associated with this article can be found, on the online version, at http://dx.doi.org/10.1016/j.jinorgbio.2014.01.019.

References

[1] H. Tapiero, K.D. Tew, Biomed. Pharmacother. 57 (2003) 399–411.
[2] N. Farrell, Coord. Chem. Rev. 232 (2002) 1–4.
[3] B.L. Vallee, D.S. Auld, Biochemistry 32 (1993) 6493–6500.
[4] G. Parkin, Chem. Commun. (2000) 1971–1985.
[5] H. Sakurai, Y. Kojima, Y. Yoshikawa, K. Kawabe, H. Yasui, Coord. Chem. Rev. 226 (2002) 187–198.
[6] C.F. Mills, Zinc in Human Biology, Springer, New York, 1989.
[7] M. Di Vaira, C. Bazzicalupi, P. Orioli, L. Messori, B. Bruni, P. Zatta, Inorg. Chem. 43 (2004) 3795–3797.
[8] Z.Q. Li, F.J. Wu, Y. Gong, C.W. Hu, Y.H. Zhang, M.Y. Gan, Chin. J. Chem. 25 (2007) 1809–1814.
[9] J. d'Angelo, G. Morgant, N.E. Ghermani, D. Desmaele, B. Fraisse, F. Bonhomme, E. Dichi, M. Sghaier, Y. Li, Y. Journaux, J.R.J. Sorenson, Polyhedron 27 (2008) 537–546.
[10] Q. Zhou, T.W. Hambley, B.J. Kennedy, P.A. Lay, P. Turner, B. Warwick, J.R. Biffin, H.L. Regtop, Inorg. Chem. 39 (2000) 3742–3748.
[11] N.C. Kasuga, K. Sekino, M. Ishikawa, A. Honda, M. Yokoyama, S. Nakano, N. Shimada, C. Koumo, K. Nomiya, J. Inorg. Biochem. 96 (2003) 298–310.
[12] A. Tarushi, Z. Karaflou, J. Kljun, I. Turel, G. Psomas, A.N. Papadopoulos, D.P. Kessissoglou, J. Inorg. Biochem. 128 (2013) 85–96.
[13] M. Belicchi Ferrari, F. Bisceglie, G. Pelosi, P. Tarasconi, R. Albertini, S. Pinelli, J. Inorg. Biochem. 87 (2001) 137–147.
[14] Z. Travnicek, V. Krystof, M. Sipl, J. Inorg. Biochem. 100 (2006) 214–225.
[15] J.S. Casas, E.E. Castellano, M.D. Couce, J. Ellena, A. Sanchez, J. Sordo, C. Taboada, J. Inorg. Biochem. 100 (2006) 124–132.
[16] K. Klein, Cosmet. Toiletries 107 (1992) 45–64.
[17] T. Hayashi, Y. Okamoto, K. Ueda, N. Kojima, Toxicol. Lett. 167 (2006) 1–7.
[18] T. Suzuki, S. Kitamura, R. Khota, K. Sugihara, N. Fujimoto, S. Ohta, Toxicol. Appl. Pharmacol. 203 (2005) 9–17.
[19] J. Chen, C. Ting, T. Hwang, L. Chen, J. Nat. Prod. 72 (2) (2009) 253–258.
[20] T.D. Venu, S. Shashikanth, S.A. Khanum, S. Naveen, A. Firdouse, M.A. Sridhar, J.S. Prasad, Bioorg. Med. Chem. 15 (2007) 3505–3514.
[21] K. Kohring, J. Wiesner, M. Altenkamper, J. Sakowski, K. Silber, A. Hillebrecht, P. Haebel, H.M. Dahse, R. Ortmann, H.J. Priv.-Doz, G. Klebe, M. Schlitzer, ChemMedChem 3 (2008) 1217–1231.
[22] J.S. Neves, L.P. Coelho, R.S. Cordeiro, M.P. Veloso, P.M. Silva, M.H. Dos Santos, M.A. Martins, Planta Med. 73 (2007) 644–649.
[23] J.J. Chen, C.W. Ting, I.S. Chen, C.F. Peng, W.T. Huang, Y.C. Su, S.C. Lin, Planta Med. 74 (2008) 1042–1051.
[24] R.G. Ferris, R.G. Hazen, G.B. Roberts, M.H. Clair, J.H. Chan, K.R. Romines, G.A. Freeman, J.H. Tidwell, L.T. Schaller, J.R. Cowan, S.A. Short, K.L. Weaver, D.W. Selleseth, K.R. Moniri, L.R. Boone, Antimicrob. Agents Chemother. 203 (2005) 4046–4051.
[25] J.P. Liou, C.W. Chang, J.S. Song, Y.N. Yang, C.F. Yeh, H.Y. Tseng, Y.K. Lo, Y.L. Chang, C.M. Chang, H.P. Hsieh, J. Med. Chem. 45 (2002) 2556–2662.
[26] Z. Wang, H.J. Lee, L. Wang, Pharm. Res.-Dord. 26 (2009) 1140–1148.
[27] R.W. Fuller, J.W. Blunt, J.L. Boswell, J. Nat. Prod. 62 (1999) 130–132.
[28] M.I. Esteva, K. Kettler, C. Maidana, J. Med. Chem. 48 (2005) 7186–7191.
[29] J. Ren, P. Chamberlain, A. Stamp, J. Med. Chem. 51 (2008) 5000–5008.
[30] U. Hagedorn-Leweke, B. Lippold, Pharmacol. Res. 12 (1995) 1354–1360.
[31] M.C. Rhodes, J.R. Bucher, J.C. Peckham, G.E. Kissling, M.R. Hejtmancik, R.S. Chhabra, Food Chem. Toxicol. 45 (2007) 843–851.
[32] S. Schauder, H. Ippen, Contact Dermatitis 37 (1997) 221–232.
[33] A. Zianna, G. Psomas, A. Hatzidimitriou, E. Coutouli-Argyropoulou, M. Lalia-Kantouri, J. Inorg. Biochem. 127 (2013) 116–126.
[34] M. Lalia-Kantouri, C.D. Papadopoulos, A.G. Hatzidimitriou, M.P. Sigalas, M. Quiros, S. Skoulika, Polyhedron 52 (2013) 1306–1316.
[35] C.D. Papadopoulos, A.G. Hatzidimitriou, M. Quiros, M.P. Sigalas, M. Lalia-Kantouri, Polyhedron 30 (2011) 486–496.
[36] M. Lalia-Kantouri, M. Gdaniec, T. Choli-Papadopoulou, A. Badounas, C.D. Papadopoulos, A. Czapik, G.D. Geromichalos, D. Sahpazidou, F. Tsitouroudi, J. Inorg. Biochem. 117 (2012) 25–34.
[37] M. Lalia-Kantouri, T. Dimitriadis, C.D. Papadopoulos, M. Gdaniec, A. Czapik, A.G. Hatzidimitriou, Z. Anorg. Allg. Chem. 635 (2009) 2185–2190.
[38] B. Armitage, Chem. Rev. 98 (1998) 1171–1200.
[39] M.J. Clarke, Coord. Chem. Rev. 232 (2002) 69–93.
[40] B.M. Zeglis, V.C. Pierre, J.K. Barton, Chem. Commun. (2007) 4565–4579.
[41] Y.K. Yan, M. Melchart, A. Habtemariam, P.J. Sadler, Chem. Commun. (2005) 4764–4776.
[42] E. Kimura, Chem. Rev. 104 (2004) 769–787.
[43] F. Dimiza, A.N. Papadopoulos, V. Tangoulis, V. Psycharis, C.P. Raptopoulou, D.P. Kessissoglou, G. Psomas, Dalton Trans. 39 (2010) 4517–4528.
[44] A. Zianna, S. Vecchio, M. Gdaniec, A. Czapik, A. Hatzidimitriou, M. Lalia-Kantouri, J. Therm. Anal. Calorim. 112 (2013) 455–464.
[45] Agilent Technologies, Program CrysAlis PRO, Ver.1.171.35, Yarnton, Oxfordshire, England, 2011.
[46] M.C. Burla, R. Caliandro, M. Camalli, B. Carrozzini, G.L. Cascarano, L. De Caro, C. Giacovazzo, G. Polidori, R. Spagna, J. Appl. Crystallogr. 38 (2005) 381–388.
[47] G.M. Sheldrick, Acta Crystallogr. A64 (2008) 112–122.
[48] L.J. Farrugia, J. Appl. Crystallogr. 30 (1997) 565.
[49] C.F. Macrae, P.R. Edgington, P. McCabe, E. Pidcock, G.P. Shields, R. Taylor, M. Towler, J. van de Streek, J. Appl. Crystallogr. 39 (2006) 453–457.
[50] R.M. Silverstein, G.C. Bassler, G. Morvill, Spectrometric Identification of Organic Compounds, 6th ed. Wiley, New York, 1998.
[51] K. Nakamoto, Infrared and Raman Spectra of Inorganic and Coordination Compounds, Part B: Applications in Coordination, Organometallic, and Bioinorganic Chemistry, 6th ed. Wiley, New Jersey, 2009.
[52] A. Tarushi, C.P. Raptopoulou, V. Psycharis, A. Terzis, G. Psomas, D.P. Kessissoglou, Bioorg. Med. Chem. 18 (2010) 2678–2685.
[53] E.K. Efthimiadou, M. Katsarou, Y. Sanakis, C.P. Raptopoulou, A. Karaliota, N. Katsaros, G. Psomas, J. Inorg. Biochem. 100 (2006) 1378–1388.
[54] F. Dimiza, A.N. Papadopoulos, V. Tangoulis, V. Psycharis, C.P. Raptopoulou, D.P. Kessissoglou, G. Psomas, J. Inorg. Biochem. 107 (2012) 54–64.
[55] A. Tarushi, F. Kastanias, V. Psycharis, C.P. Raptopoulou, G. Psomas, D.P. Kessissoglou, Inorg. Chem. 51 (2012) 7460–7462.
[56] R. Mitra, M.W. Peters, M.J. Scott, Dalton Trans. (2007) 3924–3935.
[57] D.K. Garner, S.B. Fitch, L.H. McAlexander, L.M. Bezold, A.M. Arif, L.M. Berreau, J. Am. Chem. Soc. 124 (2002) 9970–9971.
[58] P.S. Binil, M.R. Anoop, S. Suma, M.R. Sudarsanakumar, J. Therm. Anal. Calorim. 112 (2013) 913–919 (and references therein).
[59] A. Tarushi, K. Lafazanis, J. Kljun, I. Turel, A.A. Pantazaki, G. Psomas, D.P. Kessissoglou, J. Inorg. Biochem. 121 (2013) 53–65.
[60] A. Dziewulska-Kulaczkowska, J. Therm. Anal. 101 (2010) 19–26.
[61] L.M. Dianu, A. Kriza, A.M. Musuc, J. Therm. Anal. Calorim. 112 (2013) 585–593.
[62] Q. Zhang, J. Liu, H. Chao, G. Xue, L. Ji, J. Inorg. Biochem. 83 (2001) 49–55.
[63] E.C. Long, J.K. Barton, Acc. Chem. Res. 23 (1990) 271–273.
[64] A.M. Pyle, J.P. Rehmann, R. Meshoyrer, C.V. Kumar, N.J. Turro, J.K. Barton, J. Am. Chem. Soc. 111 (1989) 3053–3063.
[65] E.S. Koumousi, M. Zampakou, C.P. Raptopoulou, V. Psycharis, C.M. Beavers, S.J. Teat, G. Psomas, T.C. Stamatatos, Inorg. Chem. 51 (2012) 7699–7710.
[66] C. Tolia, A.N. Papadopoulos, C.P. Raptopoulou, V. Psycharis, C. Garino, L. Salassa, G. Psomas, J. Inorg. Biochem. 123 (2013) 53–65.
[67] G. Pratviel, J. Bernadou, B. Meunier, Adv. Inorg. Chem. 45 (1998) 251–262.
[68] A. Wolfe, G. Shimer, T. Meehan, Biochemistry 26 (1987) 6392–6396.
[69] A. Dimitrakopoulou, C. Dendrinou-Samara, A.A. Pantazaki, M. Alexiou, E. Nordlander, D.P. Kessissoglou, J. Inorg. Biochem. 102 (2008) 618–628.
[70] J.L. Garcia-Gimenez, M. Gonzalez-Alvarez, M. Liu-Gonzalez, B. Macias, J. Borras, G. Alzuet, J. Inorg. Biochem. 103 (2009) 923–934.
[71] W.D. Wilson, L. Ratmeyer, M. Zhao, L. Strekowski, D. Boykin, Biochemistry 32 (1993) 4098–4104.
[72] S. Dhar, M. Nethaji, A.R. Chakravarty, J. Inorg. Biochem. 99 (2005) 805–812.
[73] G. Psomas, J. Inorg. Biochem. 102 (2008) 1798–1811.
[74] F. Dimiza, F. Perdih, V. Tangoulis, I. Turel, D.P. Kessissoglou, G. Psomas, J. Inorg. Biochem. 105 (2011) 476–489.